Geoderma 469 (2026) 117824

Contents lists available at ScienceDirect

Geoderma

journal homepage: www.elsevier.com/locate/geoderma

Spatial and temporal resolution effects on object-based mapping of termite mounds

M.G. Maponya [a,b,*], Z.E. Mashimbye [a], C.E. Clarke [a], M.A. Cho [c]

[a] Stellenbosch University, Department of Geography and Environmental Studies, Private Bag X1 Matieland, 7602, South Africa
[b] University of Venda, Department of Geography and Environmental Sciences, Private Bag X5050, Thohoyandou 0950, South Africa
[c] Natural Resources and Environment Unit, The Council for Scientific and Industrial Research CSIR, PO Box 395 Pretoria, South Africa

ARTICLE INFO

Handling Editor: Dr Budiman Minasny

Keywords:
Termite mounds (*heuweltjies*)
Geographic Object-Based Image Analysis
Support Vector Machines
Spatial resolution
Temporal resolution

ABSTRACT

Biogenic mounds play a crucial role in shaping soil salinity patterns, carbon storage, nutrient redistribution, and rangeland functioning, making accurate information on their spatial distribution essential for effective ecosystem management. This study investigates the impact of spatial and temporal resolution on the mapping accuracy of termite mounds using remote sensing imagery. Mapping performance was evaluated using object-based image analysis combined with machine learning across multi-resolution datasets, including GeoEye-1, aerial imagery, and Sentinel-2. Two experimental designs were implemented to quantify resolution-driven differences in detection accuracy. The first set of experiments evaluated the effect of temporal resolution with 1) a seasonal Sentinel-2 image composite (June to August 2019), 2) a monthly Sentinel-2 image composite (June 2019), and 3) a single date Sentinel-2 image (June 2019). The second set of experiments assessed the impact of spatial resolution using 1) Geoeye-1 imagery, 2) aerial imagery, and 3) Sentinel-2 imagery. Classification results were analysed by comparing overall accuracies (OA) and kappa coefficients, with McNemar's test used to assess the statistical significance of accuracy differences among experiments. Results indicated that very high spatial resolution images (Geoeye-1 and aerial) based on GEOBIA and SVM allow for the classification of termite mounds with accuracies exceeding 95%. Although lower spatial resolution evidently decreased classification accuracy, increasing temporal resolution can minimise these limitations. This is demonstrated by the 10.4% and 10.8% improvements in overall accuracy (OA) using seasonal (91.1%) and monthly (90.7%) Sentinel-2 composites compared to a single-date Sentinel-2 image (80.3%).

1. Introduction

Amongst the below-ground biota, soil ecosystem engineers play a pivotal role in regulating energy and material fluxes across different spatial and temporal scales. A significant outcome of this soil engineering activity is the formation of unique, regularly spaced mounds distributed across specific landscapes (De Oliveira-Filho, 1992; Naylor et al., 2002; Sales et al., 2021). Mounds can be classified as either biogenic or non-biogenic based on their formation (Jones, 2012; Jaworski and Chutkowski, 2015; Sales et al., 2021). While non-biogenic mounds are intriguing for archaeological and geomorphological interpretations, biogenic mounds often exhibit biological, physical, and chemical heterogeneity, resulting in distinct vegetation patterns (De Freitas et al., 2021). This is particularly true for biogenic mounds that occupy the landscape along the west coast of South Africa. These mounds, locally called *heuweltjies,* contribute significantly to ecosystem species diversity (Picker et al., 2007; McAuliffe et al., 2019).

Heuweltjies typically exhibit soils with distinctive characteristics, such as increased water-holding capacity, enriched nutrient content, elevated organic carbon levels, and varied crop responses compared to surrounding soils. Clarke et al. (2022) highlighted their disproportionate contribution to carbon stocks and their association with groundwater salinisation in arid regions. Additionally, functioning as nutrient hotspots with high water-holding capacity (Midgley and Hoffman, 1991; Kunz et al., 2012), they support denser and more palatable vegetation (Bekker et al., 2016), which in turn attracts specific grazing animals, drawing carnivores (Donovan et al., 2001). Furthermore, animals that feed on the biological agents involved in mound formation concentrate around the *heuweltjies*, thereby exerting an additional influence on ecosystem dynamics (Levick et al., 2010; Mali et al., 2018).

* Corresponding author.
E-mail address: Grace.Maponya@univen.ac.za (M.G. Maponya).

https://doi.org/10.1016/j.geoderma.2026.117824
Received 15 January 2026; Received in revised form 14 April 2026; Accepted 15 April 2026
Available online 19 April 2026

Consequently, information on the spatial extent and density of *heuweltjies* is paramount for salinity and carbon modelling, nutrient hotspot mapping, rangeland management, effective ecosystem management, and other pertinent applications.

Despite the significant role played by *heuweltjies,* there is a notable gap in understanding their spatial distribution and density, which are critical factors for comprehending their impact. Apart from the study conducted by Cramer et al. (2017), which investigated the distribution of *heuweltjies* to determine the role of the Southern Harvester termite (*Microhodotermes viator*) in their formation, little has been done to address this gap. Remote sensing technology has emerged as a promising avenue for this purpose. The efficacy of remote sensing classification heavily relies on the chosen classification paradigm, algorithm, and remote sensing data (Myburgh and Van Niekerk, 2013). Numerous studies have showcased the superiority of geographic object-based image analysis (GEOBIA) approaches over traditional pixel-based methods, particularly in analysing high spatial-resolution data (Whiteside et al., 2011; Makinde et al., 2016; Piazza et al., 2016). GEOBIA refers to a category of digital remote sensing image analysis approaches that study geographic entities or phenomena by delineating and analysing image objects generated through image segmentation rather than individual pixels (Hay and Castilla, 2008; Blaschke, 2010).

Generally, object-based classification follows two approaches. Objects generated through image segmentation can either be classified using a rule-based procedure or machine learning algorithms based on training samples. Although rule-based procedures based on expert knowledge have been greatly explored, the success of these approaches depends on the operator's experience and expertise with the objects of interest (Abraham, 2005; Hamedianfar and Shafri, 2014). Therefore, in instances where the operator has limited experience and expertise, expert knowledge approaches cannot be used. This led many studies to opt for machine learning instead (Singh et al., 2016).

Machine learning algorithms have been favoured for their capacity to utilise known data for classifying large sets of imagery while integrating ancillary spatial data for detailed object classifications (Hamedianfar and Shafri, 2014; Talukdar et al., 2020). Despite ongoing advancements in machine learning algorithms, algorithms such as Support Vector Machine (SVM) have demonstrated successful applications in classifying remote sensing data. The ability of SVM to discriminate subtle differences makes it well-suited for distinguishing *heuweltjies* from the surrounding matrix. Given the high within-class variability of *heuweltjies* and their occurrence within heterogeneous landscapes, class separability is often challenging. SVM addresses this by identifying an optimal separating hyperplane that maximises class distinction, even in complex feature spaces. Its strong performance with limited, potentially imbalanced training data is particularly advantageous, given the spatially discrete and uneven distribution of *heuweltjies*. Additionally, the use of kernel functions enables the modelling of non-linear relationships between mounds and their surrounding environment, further enhancing detection. These characteristics make SVM a robust and appropriate classifier for accurate heuweltjie mapping (Khatami et al., 2016; Maxwell et al., 2018; Adugna et al., 2022).

In addition to the classification paradigm and algorithm, selecting a suitable remote sensing dataset is pivotal for effective mapping. Various remote sensing datasets, comprising multispectral data with low spatial but high temporal resolution, have been utilised for land feature mapping (Liu et al., 2013; Hao et al., 2015; Zheng et al., 2015). While these images have proven effective in mapping land features, such as archaeological mounds, their low spatial resolution limits their ability to provide detailed information about smaller land features, such as *heuweltjies* (Menze and Ur, 2012). However, the recent deployment of Sentinel-2, which provides 10-meter spatial resolution imagery at five-day intervals, represents a significant technological advancement and opens up numerous possibilities for mapping detailed land features, including micro-morphological features such as *heuweltjies* (Inglada et al., 2016; McAllister et al., 2022).

Very high-resolution commercial satellites such as Geoeye-1 are also available for purchase. Numerous researchers have investigated the use of these high-resolution images for detailed studies of land features. For instance, Lim et al. (2021) employed a combination of Geoeye-1, unmanned aerial vehicles (UAVs), and geophysical surveys to identify anomalies in archaeology. They observed that features within the 1–10 m range could be discerned using Geoeye-1 imagery. Casana and Panahipour (2014) also utilised Geoeye-1 and Worldview imagery for monitoring looting and damage at archaeological sites. They found that while the selected imagery enabled successful identification and monitoring of damaged areas, geographical and temporal inconsistencies, along with acquisition costs, posed limitations to their use.

Aerial remote sensing offers a more cost-effective alternative for monitoring and analysing the distribution of *heuweltjies* because they are freely available in South Africa. The National Geo-Spatial Information (NGI) of the Department of Agriculture, Rural Development and Land Reform has been collecting aerial imagery at a very high spatial resolution of 0.25 m in the visible (Red, Green & Blue), and Colour Infrared (CIR) regions since 2017 (Ngcofe and Semoli, 2022). These advancements in sensor technology, combined with geographic object-based image classification using machine learning, provide unprecedented capabilities for mapping small features. However, even with these advancements, a considerable need remains to explore and harness the applicability of remote sensing approaches in mapping *heuweltjies*.

The detectability of *heuweltjies* is governed by the interaction between their ecological characteristics, geomorphological expression, and the spatial and temporal properties of remotely sensed data. Ecologically, *heuweltjies* function as nutrient- and moisture-enriched hotspots that support denser and more persistent vegetation than the surrounding matrix, resulting in distinct spectral signatures. Geomorphologically, they occur as subtle, circular micro-topographic mounds that can be characterised using terrain derivatives such as topographic position, slope, and curvature. The extent to which these ecological and structural signals are captured is strongly influenced by sensor resolution. While very high-resolution imagery enables the direct detection of both vegetation contrast and mound morphology, medium-resolution imagery such as Sentinel-2 may be constrained by pixel mixing. Nevertheless, the integration of multi-temporal composites and terrain data can enhance detectability by reinforcing both spectral and topographic distinctions, thereby compensating for spatial limitations.

Despite their ecological significance, studies employing remote sensing to map *heuweltjies* remain limited, and the influence of spatial and temporal resolution on mapping accuracy is not yet well understood. Furthermore, the effectiveness of GEOBIA for detecting and mapping heuweltjies has not been fully established. This study therefore posits the following hypotheses: (1) the application of GEOBIA will improve detection accuracy by leveraging the distinct shape and contextual contrast of heuweltjies; (2) the pronounced spectral and morphological characteristics of heuweltjies enable accurate mapping using high- to very high-resolution imagery; (3) incorporating phenological variability will enhance detection accuracy when using remote sensing and SVM; and (4) the integration of very high-resolution terrain features will further improve detection performance.

Accordingly, this study aims to assess the influence of spatial and temporal resolution on the mapping accuracy of heuweltjies using a GEOBIA–SVM framework. Multi-source datasets, including high-resolution Sentinel-2 imagery, very high-resolution aerial imagery, and GeoEye-1 data, are utilised. A range of features, including spectral bands, vegetation indices, terrain variables, and textural attributes, are derived and integrated as inputs for classification. The findings are interpreted in the context of developing a robust and scalable methodology for detecting and mapping the spatial distribution of biogenic mounds, such as heuweltjies, using GEOBIA and remote sensing data.

2. Materials and methods

2.1. Study Site

This study was conducted south of Komaggas, a town in the Namakwa District Municipality, Northern Cape Province, South Africa (Fig. 1). This area, densely packed with *heuweltjies*, is located approximately 40 km southwest of Springbok and 45 km north of Soebatsfontein on the Komaggas River tributary of the Buffels. The study area is located in a semi-arid region with winter rainfall, characterised by a mean annual precipitation range of 50 mm to 400 mm per annum. Over 60% of the rain falls between May and September due to the cold, westerly fronts from the southern oceans (Davis et al. 2016). Annual average temperatures for the area range from 13 °C to 21 °C, owing to the cold Benguela Current off the west coast. Maximum temperatures only exceed 30 °C when Berg winds blow off the plateau to the west (Conway et al., 2015).

Generally, the Komaggas area experiences relatively high evaporative demand, particularly during the hot berg-wind incidents. The predominant regional biome is the Succulent Karoo, characterised by the Namaqualand heuweltjieveld, which has relatively rich soils derived from underlying granite or gneiss. The vegetation cover comprises a mosaic of low shrubland communities dominated by leaf-succulent shrubs on the mounds, ascribed to the activity of harvester termites. This study area was chosen owing to the availability of (i) quality satellite and aerial images; and (ii) pristine and geomorphological properties of the study site, which make the *heuweltjies* highly visible in digital elevation models, aerial, and satellite images. The extent of the study area was chosen to coincide with a Geoeye-1 satellite image scene.

2.2. Data acquisition and pre-processing

A single-date Geoeye-1 image, Sentinel-2 imagery, aerial imagery, and a digital elevation model (DEM) were used in this study (Table 1 and Fig. 2). Each of these datasets is described in the following subsections.

Table 1
Data sources and their respective spatial resolutions.

Sensor name	Spectral bands	Spatial resolution
GeoEye-1	Blue, green, red near-infrared, panchromatic band	2 *m* 0.5 *m*
Aerial imagery – RGB	Blue, green, red	0.5 *m*
Aerial imagery – CIR	NIR, red, blue	0.5 *m*
Sentinel-2	Blue, green, red, NIR Vegetation red edge (3) narrow NIR, SWIR (2) Coastal aerosol, water vapor, SWIR	10 *m* 20 *m* 60 *m*
DEMSA	Single band	2 *m*

2.2.1. Geoeye-1

A single date atmospherically corrected Geoeye-1 image, collected in June 2019, covering the test site, was purchased from Geo Data Design (Pty) Ltd (https://geodatadesign.co.za/). Geoeye-1 sensors collect imagery at 0.5 m and 2 m spatial resolution for the panchromatic and multispectral bands, respectively. These sensors measure reflected radiance in four (4) multispectral bands (visible and near-infrared) and a panchromatic band. However, for this analysis, only the visible and near-infrared bands were considered.

2.2.2. Aerial imagery

Very high-resolution (0.25 m) aerial imagery covering the study site was obtained from the National Geo-spatial Information (NGI) to test the feasibility of using the developed approach with freely available imagery. The NGI has been providing aerial photographs at a national scale since the 1950 s. Following the global trend towards digital image acquisition in 2005, the NGI introduced an Intergraph Digital Mapping Camera (I-DMC). From 2008 to 2016, colour digital aerial imagery was collected with a spatial resolution of 0.5 m, and from 2017 to the present, with a resolution of 0.25 m. Currently, the 12-bit aerial images are collected in true colour (RGB), colour infrared (CIR), and panchromatic bands. While the true colour images cover the blue, green, and red

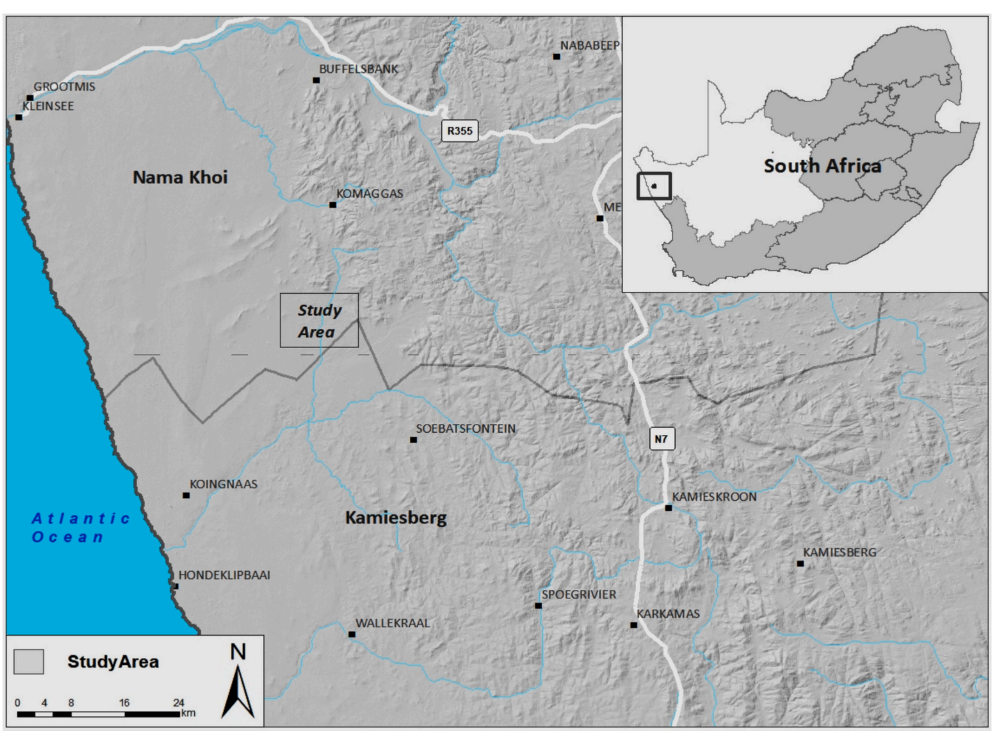

Fig. 1. Location of the study area in the Northern Cape, South Africa.

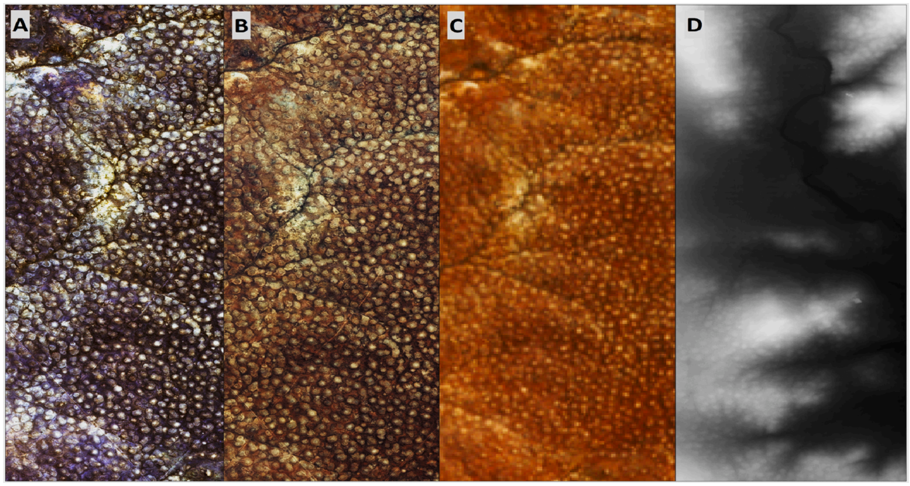

Fig. 2. The different datasets with varying spatial resolutions A) Aerial image B) Geoeye-1C) Sentinel-2 D) DEMSA.

bands, the colour infrared collects data in the near-infrared, red, and blue bands. For this study, only the RGB and near-infrared bands were used. The RGB and CIR images were composited to extract the four bands of interest (blue, green, red, and NIR). For a comprehensive explanation of the dataset, the reader is referred to Ngcofe and Semoli (2022).

2.2.3. *Sentinel-2*

An image composite of selected cloud-free Sentinel-2 images, pre-processed at Level 2A and captured from June (2019) to August (2019), representing a typical winter season in the study area, and a monthly composite of images collected in June (2019) sourced from Google Earth Engine (GEE), was used to assess the influence of temporal resolution on classification accuracies for detecting *heuweltjies*. The composites were limited to 3 months to minimise interseason variations within the study area, and the winter season was selected to coincide with the acquisition date for Geoeye-1. In addition to the image composites, a single-date Sentinel-2 image captured in June 2019 was sourced and used in conjunction with the other datasets to assess the impact of both spatial and temporal resolutions on classification accuracy. Data preparation involved stacking and resampling the 20 m spectral bands to 10 m (Immitzer et al., 2016). For the seasonal and monthly image composites, the median of the selected images was used.

2.2.4. *Digital elevation model*

The 2 m Digital Elevation Model of South Africa (DEMSA2) for the study area was obtained from the Centre of Geographical Analysis (CGA) at Stellenbosch University. DEMSA2 is extracted from 0.5 m resolution stereo aerial imagery, with a vertical accuracy of approximately 50 cm and a horizontal accuracy of approximately 1 m (Shabalala and Ekolu, 2019). DEMSA2 data was considered due to its high resolution and availability anywhere in South Africa. Although DEMSA is a commercial product, it was freely provided by the CGA for this study.

2.2.5. *Sample points collection*

Three thousand (3000) sample points, representing both on– and *off-heuweltjies*, were manually delineated from the study area using very high-resolution satellite imagery. These sample points were then joined

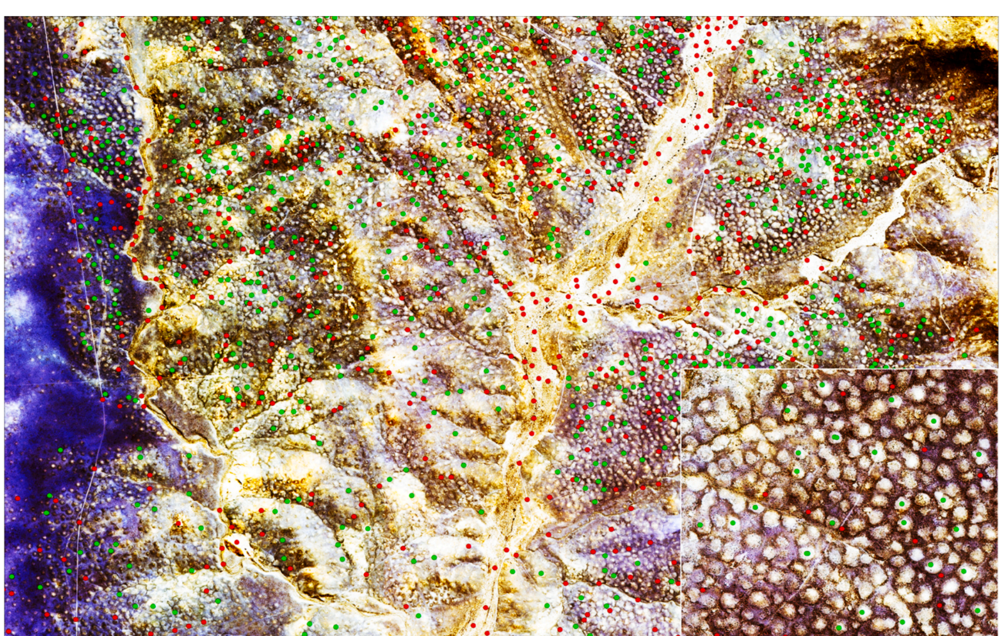

Fig. 3. Distribution of ground control points.

with the input objects generated through image segmentation (Section 2.3) using spatial joins to create training and reference object samples for image classification and statistical evaluation purposes. A total of 1500 samples representing *heuweltjies* and 1500 representing off-*heuweltjies* surfaces were collected, and the distribution of the collected samples is given in Fig. 3.

2.3. Multiresolution image segmentation

The multiresolution segmentation algorithm, a bottom-up approach that iteratively merges pixels or existing image objects into larger objects based on relative homogeneity, as implemented in Trimble eCognition, was used to segment the imagery. Due to the variability in diameter, boundary definition, and vegetation cover of *heuweltjies*, optimal segmentation parameters cannot be determined a priori. Therefore, segmentation parameters were iteratively adjusted to evaluate how effectively the resulting objects captured the morphological structure and boundaries of the mounds for each of the datasets considered in this study. This trial-and-error process facilitated the identification of parameters that balanced over- and under-segmentation, ensuring that individual *heuweltjies* were represented as discrete objects rather than fragmented or merged with surrounding features, thereby improving the reliability of the subsequent classification.

The approach was used to determine the scale, shape, and compactness parameters that defined the size and form of the segmented objects for optimal *heuweltjie* detection. A three-step hierarchical region-growing procedure was applied to RGB bands from GeoEye-1, aerial imagery, and Sentinel-2 data. All bands were assigned equal weighting (1). The scale parameter was initially set to 10 and subsequently increased to 20 and 40, while shape and compactness were fixed at 0.8 and 0.2, respectively. The same parameter set was applied across the three datasets.

2.4. Input variable generation

Forty (40) features were generated for the experiments undertaken with the Geoeye-1 and aerial imagery independently, while forty-six (46) features were generated for the experiment undertaken using Sentinel-2 imagery due to the additional number of bands offered by the Sentinel-2 mission (Table 2). A similar set of features was generated for the Sentinel-2, Geoeye-1, and aerial image analyses. For this study, the blue, green, red, and NIR bands were used for Geoeye-1 and aerial image analyses, while blue, green, red, three red edge bands, two NIR bands, and two SWIR bands were used for Sentinel-2 analysis. In addition to the bands, the generated features included eight (8) indices, eight (8) textural features Haralick and Shanmugam, 1973), and nineteen (19) terrain variables (Fisher et al., 2017) (Table 2). Spectral indices, textural features, and terrain variables were integrated with spectral bands to improve classification robustness by reducing dependence on spectral properties alone, which are subject to spatial and temporal variability.

Table 2
Variables used as input for classifications.

Variable source	Dataset	Features
Spectral bands	Geoeye-1 & Aerial images	Blue, green, red, NIR
	Sentinel-2	Blue, green, red, NIR, narrow NIR, vegetation red edge (B5, 6 & 7) SWIR (B 11 & 12)
Indices	Geoeye-1, Aerial images & Sentinel-2	Baresoil index, brightness index, coloration index, carbonate index, NDVI, NDWI, salinity index, SAVI
Textural features	Geoeye-1, Aerial images & Sentinel-2	ASM, contrast, dissimilarity, energy, entropy, mean, variance, homogeneity
Terrain attributes	Digital elevation model	Aspect, analytical hillshading, close depressions, channel network base level, channel network distance, flow line curvature, general curvature, longitudinal curvature, LS-Factor, maximal curvature, minimal curvature, plan curvature, profile curvature, relative slope position, slope, tangential curvature, total curvature, total catchment area, topographic wetness index, valley depth

2.5. Experimental design

Two sets of experiments were conducted to evaluate the influence of temporal and spatial resolutions on the classification accuracy for detecting biogenic mounds based on GEOBIA. In the first set, three experiments involving seasonal (June to August 2019) and monthly (June 2019) image composites, along with a single-date Sentinel-2 image from June 2019, were utilised to assess the effect of temporal resolution. The second set also involved three experiments utilising a Geoeye-1 image acquired in June 2019, an aerial image from 2017, and another single-date Sentinel-2 image captured in June 2019 to examine the impact of spatial resolution.

2.6. Classification and accuracy assessment

Support Vector Machines (SVM) implemented in the supervised learning and image classification environment (SLICE) software, developed by the Centre for Geographical Analysis (CGA) at Stellenbosch University, was used for classification (Myburgh and Van Niekerk, 2013). SLICE incorporates several classification algorithms, including SVM, k-NN, DT, RF, and ML, but for this study, only SVM was considered. The SVM classifier in SLICE was implemented using Libsvm 3.0 (Chang and Lin, 2011). The shapefiles were manipulated using the Geospatial Data Abstraction Library (GDAL). The Geospatial Data Abstraction Library (GDAL) was used to manipulate raster and shapefile data. For a trenchant description of the classifier configuration, refer to Myburgh and Van Niekerk (2013).

SLICE was also used for accuracy assessment, and a 3:2 sample split ratio was employed for training and statistical evaluation, i.e., 40% of the samples were randomly selected and excluded from classifier training. The excluded samples were used to validate the classifications independently. The same set of training and statistical evaluation samples was maintained for all experiments. Overall accuracy (OA) and the kappa coefficient (K) were calculated for every classification. McNemar's test, (as implemented in Microsoft Excel) was used to assess the statistical significance of the accuracy obtained from the experiments, as recommended by Foody and Mathur (2004). The alpha value for McNemar's test was set to 0.05.

3. Results

Fig. 4 illustrates the results of image segmentations performed on the various datasets. The influence of segmentation outputs on subsequent classification accuracies is apparent from both the segmentation results and classification outcomes. The multiresolution segmentation algorithm was applied to different datasets (Geoeye-1, aerial, and Sentinel-2 images) to produce image objects delimiting *heuweltjies*. Geoeye-1 and aerial images with RGB bands assigned a similar weighting of one, and a hierarchical segmentation with region merging at different scales produced satisfactory delimitations of the mounds, yielding comparable numbers of image objects. The segmentation of the aerial and Geoeye-1 images yielded a total of 106,015 and 118,480 image objects, respectively. In contrast, Sentinel-2 imagery segmentation produced significantly fewer objects (a total of 31,449) using the same segmentation parameters.

As can be observed in Fig. 4, segmentation results based on Geoeye-1 and aerial imagery appeared to follow the boundaries of *heuweltjies*

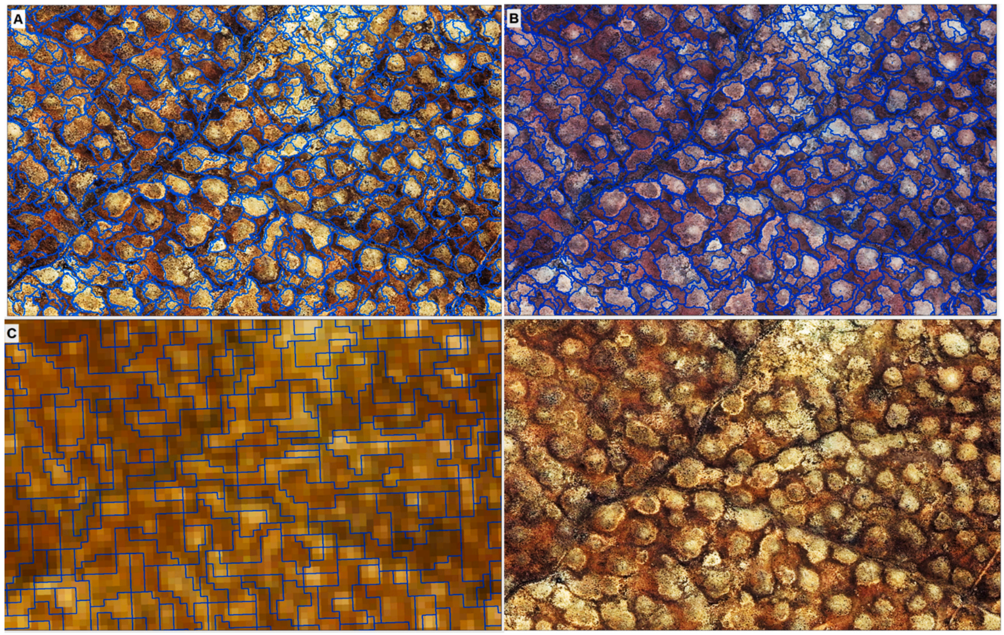

Fig. 4. Segmentation outputs for the different datasets (A) Aerial image, (B) Geoeye-1, and (C) Sentinel-2 and Aerial image without segments.

closely, while those based on Sentinel-2 did not align well with the boundaries. Overall, segmentation quality corresponded closely with the spatial resolution of the imagery. Geoeye-1 imagery (2 m) produced well-defined, compact objects that accurately reflected the boundaries of individual features. Aerial imagery, with even finer resolution (0.25 m), generated coherent segments with precise feature detection. In contrast, Sentinel-2 imagery (10 m) produced larger, less distinct segments that often merged adjacent features or missed small-scale variability. These results highlight that higher-resolution data enable more accurate segmentation, which in turn improves classification outcomes.

Results on the impact of temporal resolution on the detection of *heuweltjies* are presented in Table 3 and Fig. 5. The experiment conducted using the seasonal image composite achieved an Overall Accuracy (OA) of 91.1%. This OA was only slightly higher (<0.4%) than that obtained with the monthly image composite (90.7%). Conversely, the classification of *heuweltjies* based on a single date Sentinel-2 image yielded the lowest OA of 80.3%. The high OA (91%) and PA (93%) achieved with the seasonal classification indicate that most samples were correctly identified with minimal omission error. However, the slightly lower user's accuracy (89%) suggests the presence of some commission error, which explains the generalisation observed in Fig. 5. In comparison, the monthly image composite produced similarly high OA (90%) and UA (87%), but a lower PA (82%). This pattern indicates that, although overall classification performance remained strong, omission error increased relative to the seasonal classification, while commission error decreased slightly.

Together, these results suggest that seasonal compositing improves class detection, whereas monthly compositing yields marginally purer class assignments but at the cost of increased missed instances. This is further evident in the Kappa coefficients for the seasonal (0.81) and monthly (0.80) classifications, indicating strong agreement between the classified outputs and the reference data beyond chance. Contrary to the seasonal and monthly classifications, the lower Kappa coefficient (0.60) for the single-date classification suggests a rather moderate agreement between the classification and reference data, further demonstrating the impact of temporal resolution on the classification accuracy of *heuweltjies*.

While the disparity in OAs between the seasonal and monthly composites is only marginal, both image composites exhibited significantly better performance ($P < 0.007$) compared to the single-date image. Upon visual inspection of the classification outcomes, it becomes apparent that both monthly and single-date imagery tend to overestimate the presence of *heuweltjies* (see Fig. 5). Contrary to the statistical analysis, Fig. 5 indicates that none of the classifications accurately delineated the boundaries of *heuweltjies*. This limitation is attributed to the lower spatial resolution of Sentinel-2 imagery. *Heuweltjies* are relatively small features, making it challenging to precisely classify them using Sentinel-2 imagery. However, it is noteworthy that temporal resolution appears to impact the accuracy of *heuweltjies* classification using GEOBIA, with higher temporal resolution enhancing their detection.

The results illustrating the influence of spatial resolution on the classification accuracy of *heuweltjies* are presented in Table 4 and Fig. 6. In this experiment, the highest OA of 96.7% was achieved using GeoEye-1 imagery, followed by aerial imagery (95.3%) and Sentinel-2 (80.3%). The high OAs (>95%) obtained for the aerial and GeoEye-1 datasets are supported by high producer's accuracies (PA ≈ 96%) and user's accuracies (UA > 95%), indicating low omission and commission errors and strong class-level performance. In contrast, the Sentinel-2 classification yielded lower PA and UA values (84% and 83%, respectively), reflecting comparatively higher error rates, as illustrated in Fig. 6. The Kappa coefficients further support these findings: aerial imagery (0.90) and GeoEye-1 imagery (0.94) indicate almost perfect agreement between the classified outputs and reference data, while Sentinel-2 (0.60) demonstrates moderate agreement.

Although there is a slight difference in the OAs (~1.4%) obtained with Geoeye-1 and aerial images, the difference is statistically insignificant ($P > 0.34$). In contrast, both Geoeye-1 and aerial imagery significantly outperformed Sentinel-2 ($P < 0.007$). As shown in Fig. 6, classification using Geoeye-1 and aerial imagery appears to delineate the boundaries of *heuweltjies* more accurately than Sentinel-2 imagery.

Table 3
Overall Accuracies (OAs) and Kappa coefficients (K) for the different experiments, undertaken with SVM and A) Sentinel-2 seasonal image composite, B) Sentinel-2 monthly image composite, and C) Sentinel-2 single-date image to assess the impact of temporal resolution on the detection of heuweltjies.

Seasonal		Monthly		Single	
OA	K	OA	K	OA	K
91.1	0.81	90.7	0.80	80.3	0.60

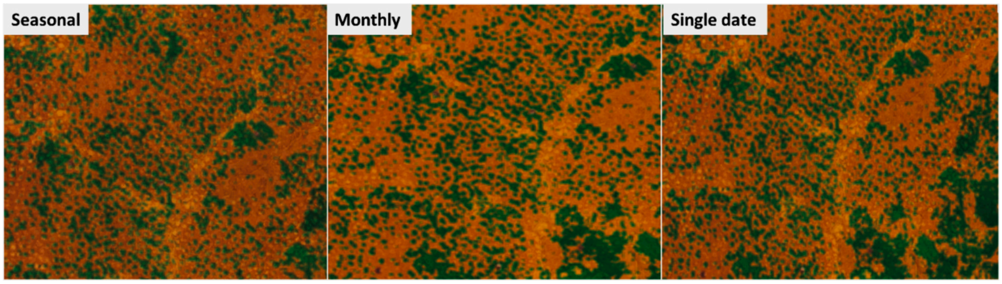

Fig. 5. Classification results for the three datasets used to assess the influence of temporal resolution on classification accuracies: A) seasonal image composite; B) monthly image composite; and C) single date image.

Table 4
Overall Accuracies (OAs) and Kappa coefficients (K) for the different experiments, undertaken with SVM and A) Aerial imagery, B) Geoeye-1 image, and C) Sentinel-2 image to assess the impact of spatial resolution on the detection of *heuweltjies*.

Aerial		GeoEye-1		Sentinel-2	
OA	K	OA	K	OA	K
95.3	0.90	96.7	0.94	80.3	0.60

The classification based on Sentinel-2 does not accurately delineate the boundaries of *heuweltjies* and tends to overestimate their distribution.

Overall, very high-resolution Geoeye-1 and aerial imagery yielded comparable and more accurate image objects that aligned closely with the boundaries of *heuweltjies*. Segmentation results based on Sentinel-2 imagery did not accurately delineate the boundaries of *heuweltjies*. While the OA and K statistics for the monthly and seasonal Sentinel-2 composites were high, these classifications tended to overestimate the distribution of *heuweltjies*. Very high-resolution Geoeye-1 and aerial imagery produced more accurate classifications of *heuweltjies*.

4. Discussion

Based on the segmentation outputs and subsequent classification results, it is evident that the quality of image segmentation directly influences the classification outcome. While it is generally agreed that image segmentation is a critical initial step in object-based classification, the assumption that segmentation output directly affects classification means that optimising segmentation results before classification clearly improves subsequent classification results. For this study, optimal segmentation refers to one that best delimits *heuweltjies* and results in the highest classification accuracy. It is clear from the resulting classifications that Geoeye-1 and aerial image-based experiments outperformed those of Sentinel-2. This result correlates directly with the image segmentation outputs for the respective experiments (See Figs. 4 and 5). This result aligns with the findings of Gao et al. (2011), who assessed the impact of segmentation on land cover classification accuracy and found that segmentation outputs significantly affect classification accuracy.

The differences in segmentation outputs across experiments are believed to have been strongly influenced by the spatial resolution of the input datasets. According to Sales et al. (2021), *heuweltjies* are wide, regularly spaced, lenticular features that range in diameter from 17 m to 30 m and in height from 1.45 m to 2.5 m. However, this analysis showed that, despite the size of the objects, very fine spatial resolution is required for efficient delimitation, leading to more accurate classifications. This is corroborated by the findings of Mesner and Oštir (2014), who investigated the impact of spectral and spatial resolution on segmentation quality and found that decreasing spatial resolution deteriorated segmentation quality, even when the objects were larger. This finding indicates that achieving high-quality segmentation for this application requires a high spatial resolution.

Regarding the datasets, the results show that Geoeye-1 and aerial

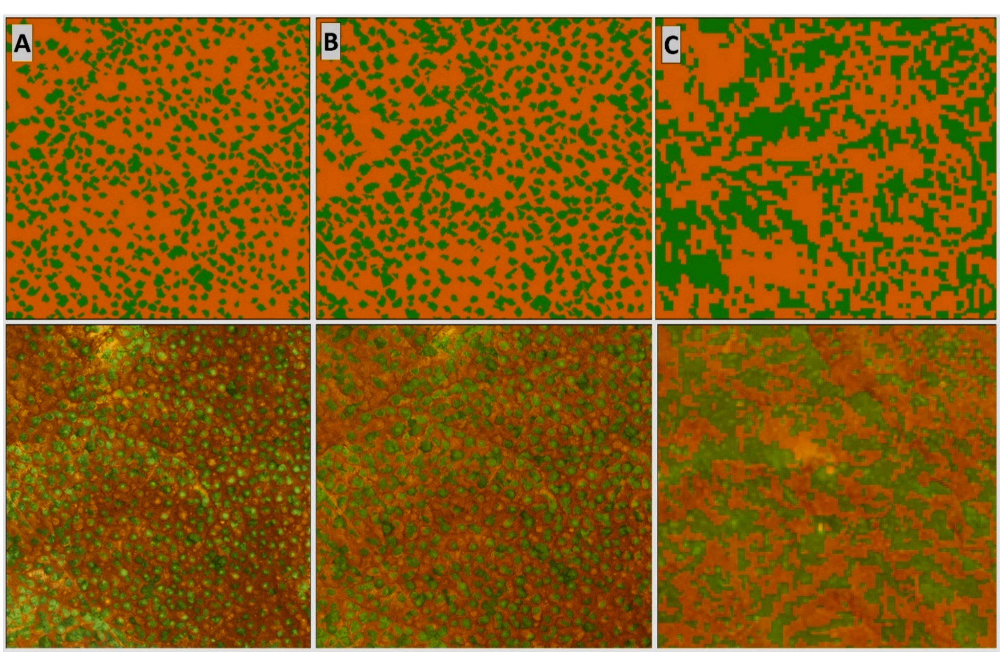

Fig. 6. Classification results with reduced transparency for the three datasets considered in this study. A) Aerial image, B) Geoeye-1, C) Sentinel-2.

images outperformed Sentinel-2. While Sentinel-2 obtained significantly lower OAs compared to Geoeye-1 and aerial images, the differences between OAs obtained with Geoeye-1 and aerial images are only marginal (diff = 1.4%). Congruent with studies by Lim et al. (2021) and Casana and Panahipour (2014), who assessed and reported on the efficacy of Geoeye-1 imagery for archaeological studies, the cost associated with its acquisition restricts its application in remote sensing studies. However, as postulated by Lovitt et al. (2017), aerial images provide a cost-effective alternative to Geoeye-1, particularly for fine-detail mapping, such as detecting *heuweltjies*, as evident from the results obtained from experiments undertaken with Geoeye-1 and aerial images. Sărășan et al. (2020) further confirmed the efficacy of aerial applications for mapping burial mounds, reporting an overall detection rate of 90%. While their study focused on only 21 foreknown burial mounds, the current study achieved an OA exceeding 90%, considering a much higher mound density in the aerial image, which was obtained without prior knowledge. This offers a strong affirmation of the potential of these images for mapping *heuweltjies*.

The difference in OAs obtained with very high versus high-resolution images betokens the importance of selecting the right remote sensing data source for a specific application. With a difference of 16.4% in OA from an 8 m spatial resolution difference and a difference of 15% with a 9.5 m spatial resolution difference, respectively, Geoeye-1 and aerial images outperformed the Sentinel-2 image. Based on these results, it is clear that for detecting *heuweltjies*, very high spatial resolution is critical, particularly when single-date images are used. However, increasing temporal resolution can help counteract the limitations encountered with lower spatial resolution. The significantly different results obtained from experiments undertaken with Sentinel-2 seasonal and monthly image composites and Sentinel-2 single-date images indicate that, although Sentinel-2 images are collected at a lower spatial resolution, the higher temporal resolution does compensate for the insufficient detail detectable by classifiers from the lower spatial resolution.

The difference of 10.4% and 10.8% in OAs achieved with a single date Sentinel-2 image (80.3%) versus the OAs achieved with the seasonal and monthly composited Sentinel-2 images (91.1% & 90.7% respectively) is a clear indication of the contribution of temporal resolution to classification accuracies. This finding aligns with the results of Yao et al. (2023), who compared data sources with varying spatial and temporal resolutions for efficient orchard mapping. By comparing single-date Worldview-2 to multitemporal Landsat-8 and Sentinel-2, they found that although with a small margin, the benefit of increasing the level of details of temporal features on accuracy is higher than that of spatial features, indicating that for their application, the classification ability of temporal information is higher than that of spatial information. It is believed that although the monthly temporal period used for image composites may be short for capturing seasonal changes on the mounds, the increase in the number of images incorporated in the classification helps minimise sensor errors found on individual images, thus improving classifier performance.

The comparable results achieved through experiments undertaken with Geoeye-1 and aerial images demonstrate that aerial images can yield results as good as those obtained with Geoeye-1. Considering the cost of the Geoeye-1 image, this finding offers an important cost-effective alternative for detecting *heuweltjies* or other biogenic mounds. Furthermore, the minor differences in OAs between experiments undertaken with Geoeye-1 and aerial images, in comparison to the significant difference in OAs achieved with both experiments undertaken with Geoeye-1 and aerial images, when compared to the experiment undertaken with Sentinel-2, indicate the importance of spatial resolution for detecting *heuweltjies*. This is particularly true when single-date images are used. However, it is also clear that with an increase in temporal resolution, high-resolution satellite images such as Sentinel-2 can effectively detect *heuweltjies*. This is an important finding because the cost of image acquisition has been a significant limitation in applying remote sensing for fine-detail mapping over large regions over the years. However, this result demonstrates that, coupled with the high temporal resolution, the high resolution offered by open-source satellite missions, such as Sentinel-2, provides an opportunity for mapping *heuweltjies* over larger areas.

Furthermore, by capturing subtle but persistent microtopographic contrasts between mound and matrix soils, terrain variables are believed to have played an important role in augmenting the detectability of *heuweltjies*. While spectral features may exhibit seasonal variability, making them susceptible to vegetation-related confounding, terrain derivatives can provide temporally stable structural information. Their inclusion is therefore believed to have improved class separability, reduced false positives associated with spectrally similar features, and enabled the model to incorporate geomorphic context alongside surface reflectance characteristics. Consequently, terrain variables are important not only for enhanced classification accuracy but also for reinforcing the importance of microrelief in defining *heuweltjie* morphology and spatial organisation across semi-arid landscapes.

These findings provide an efficient, cost-effective approach to mapping the spatial distribution of *heuweltjies* and other biogenic mounds similar to them. This information is essential for ecologists, rangeland managers, and hydrologists who need to accurately quantify the impacts of these mounds on ecological dynamics and functions, groundwater modelling, rangeland management, and nutrient hotspot mapping, among other applications. Despite the noted successes, the approach developed in this study was tested in a smaller area. Given the potential of aerial and high-temporal-resolution images, as demonstrated by freely available satellite imagery such as Sentinel-2 in this study, it would be beneficial to assess the approach on a larger scale.

The improved detection of *heuweltjies* has important implications for understanding landscape-scale soil processes. As nutrient- and organic matter-enriched microsites embedded within comparatively depleted matrix soils, *heuweltjies* function as spatially discrete biogeochemical hotspots. Enhanced mapping accuracy provides baseline support for more reliable estimates of soil organic carbon stocks and has the potential to reduce uncertainty in regional carbon budgeting. It may also provide a useful foundation for assessing salinity heterogeneity and contribute to the evaluation of competing pedogenic and biogenic formation hypotheses. At broader scales, improved spatial characterisation could inform models of nutrient redistribution, ecosystem productivity, and semi-arid landscape resilience, thereby positioning *heuweltjies* as potentially regulators of soil heterogeneity and biogeochemical cycling.

This study exclusively employed a Support Vector Machine (SVM) classifier to map the spatial distribution of *heuweltjies*. While SVM demonstrated strong performance in capturing mound–matrix separability, reliance on a single classification algorithm may limit insight into the relative advantages of alternative modelling approaches. Additionally, this study focused on a small area with relatively favourable conditions, which may not fully capture the variability inherent in *heuweltjie* landscapes; although terrain, textural, and spectral indices were used to reduce sensitivity to spatial and temporal variability, future work should test the approach in larger, more heterogeneous landscapes. Also, future research should explore and compare additional machine learning classifiers to assess potential improvements in classification accuracy, robustness, and transferability across varying environmental and seasonal conditions. A comparative framework would provide a more comprehensive evaluation of optimal modelling strategies for biogenic mound detection and enhance methodological generalisability.

5. Conclusion

This study assessed the effect of spatial and temporal resolutions on the mapping accuracy of *heuweltjies* based on GEOBIA and SVM Specifically, this study hypothesised that: 1) Leveraging GEOBIA will enhance the accuracy of delineating *heuweltjies* due to their circular shape and contrast with the surrounding environment. 2) *Heuweltjies*, owing to their distinct spectral and morphological characteristics, can be accurately mapped using high-resolution remote sensing data. 3) Utilising phenological characteristics will improve the precision of *heuweltjies* detection. 4) Integration of very high-resolution terrain features will augment the detection of *heuweltjies*. The results show that:

1. In the case of single-date remote sensing datasets, this study found that utilising very high spatial resolution images, such as GeoEye-1 and aerial imagery, can accurately map *heuweltjies*, achieving overall accuracy exceeding 95%.
2. Leveraging phenological characteristics by increasing the temporal resolution for experiments conducted with Sentinel-2 images improved classification accuracy by over 10%.
3. There exists a direct correlation between segmentation outputs and subsequent classification results. Therefore, GEOBIA does enhance the detectability of *heuweltjies*.
4. The inclusion of terrain variables derived from very high-resolution digital elevation models is believed to have significantly contributed to the high accuracies obtained across classifications.

Based on the findings of this study, it is concluded that when assessing single-date images, spatial resolution significantly influences the accurate detection of *heuweltjies*. However, it is evident that increasing the temporal resolution, thereby augmenting phenological information available with high-resolution images such as Sentinel-2, can help minimize the limitations posed by comparatively lower spatial resolution. Additionally, leveraging objects generated through the multi-resolution image segmentation algorithm enhances subsequent classification accuracies of *heuweltjies*. Essentially, we assert that utilising either very high spatial or temporal resolution images, coupled with terrain variables derived from very high-resolution digital elevation models, alongside SVM, can effectively map *heuweltjies* and other mounds with similar morphological and spectral characteristics in areas similar to the study site considered in this research.

CRediT authorship contribution statement

M.G. Maponya: Writing – review & editing, Writing – original draft, Validation, Resources, Project administration, Methodology, Investigation, Formal analysis, Data curation, Conceptualization. **Z.E. Mashimbye:** Writing – review & editing, Conceptualization. **C.E. Clarke:** Writing – review & editing, Funding acquisition, Conceptualization. **M. A. Cho:** Conceptualization.

Declaration of competing interest

The authors declare the following financial interests/personal relationships which may be considered as potential competing interests: DR MG MAPONYA reports financial support was provided by South African National Research Foundation (Grant Number 118594). DR MG MAPONYA reports financial support was provided by DSTNRF iPhakade program. If there are other authors, they declare that they have no known competing financial interests or personal relationships that could have appeared to influence the work reported in this paper.

Data availability

Data will be made available on request.

References

Abraham A (2005). Rule-based expert systems. *Handbook of measuring system design.*
Adugna, T., Xu, W., Fan, J., 2022. Comparison of random forest and support vector machine classifiers for regional land cover mapping using coarse resolution FY-3C images. Remote Sens. (Basel) 14 (3), 574.
Bekker, S.J., Hoffman, J.E., Jacobs, S.M., Strever, A.E., Van Zyl, J.L., 2016. Ecophysiology, vigour, berry and wine characteristics of grapevines growing on and off heuweltjies. S. Afr. J. Enol. Vitic. 37 (2), 176–192.
Blaschke, T., 2010. Object based image analysis for remote sensing. ISPRS J. Photogramm. Remote Sens. 65 (1), 2–16.
Casana, J., Panahipour, M., 2014. Satellite-based monitoring of looting and damage to archaeological sites in Syria. Journal of Eastern Mediterranean Archaeology & Heritage Studies 2 (2), 128–151.
Chang, C.C., Lin, C.J., 2011. LIBSVM: a library for support vector machines. ACM Transactions on Intelligent Systems and Technology (TIST) 2 (3), 1–27.
Clarke, C.E., Vermooten, M., Watson, A., Hattingh, M., Miller, J.A., Francis, M.L., 2022. Downward migration of salts in termite-affected soils: Implications for groundwater salinization. Geoderma 413, 115747.
Conway, D., Van Garderen, E.A., Deryng, D., Dorling, S., Krueger, T., Landman, W., Lankford, B., Lebek, K., Osborn, T., Ringler, C., Thurlow, J., 2015. Climate and Southern Africa's water–energy–food nexus. Nat. Clim. Chang. 5 (9), 837–846.
Cramer, M.D., von Holdt, J.R., Uys, V.M., Midgley, J.J., 2017. The present and likely past climatic distribution of the termite Microhodotermes Viator in relation to the distribution of heuweltjies. J. Arid Environ. 146, 35–43.
Davis, C.L., Timm Hoffman, M., Roberts, W., 2016. Recent trends in the climate of Namaqualand, a megadiverse arid region of South Africa. S. Afr. J. Sci. 112 (3–4), 1–9.
De Freitas, D.F., Ker, J.C., da Silva Filho, L.A., Pereira, T.T., de Souza, O.F., Schaefer, C.E. G., 2021. Pedogeomorphology and paleoenvironmental implications of large termite mounds at the Brazilian semiarid landscape. Geomorphology 387, 107762.
De Oliveira-Filho, A.T., 1992. Floodplain 'murundus' of Central Brazil: evidence for the termite-origin hypothesis. J. Trop. Ecol. 8 (1), 1–19.
Donovan, S.E., Eggleton, P., Dubbin, W.E., Batchelder, M., Dibog, L., 2001. The effect of a soil-feeding termite, Cubitermes fungifaber (Isoptera: Termitidae), on soil properties: termites may be an important source of soil microhabitat heterogeneity in tropical forests. Pedobiologia 45 (1), 1–11.
Fisher, R., Hobgen, S., Mandaya, I., Kaho, N.R., Kehutanan, Z.F., 2017. Satellite image Analysis and Terrain Modelling: a practical manual for natural resource management, disaster risk and development planning using free geospatial data and software. Charles Darwin University, Universitas Nusa Cendana Dan Universitas Halu Oleo: Wordpress. 2 (4), 99–102.
Foody, G.M., Mathur, A., 2004. Toward intelligent training of supervised image classifications: directing training data acquisition for SVM classification. Remote Sens. Environ. 93 (1–2), 107–117.
Gao, Y.A.N., Mas, J.F., Kerle, N., Navarrete Pacheco, J.A., 2011. Optimal region growing segmentation and its effect on classification accuracy. Int. J. Remote Sens. 32 (13), 3747–3763.
Hamedianfar, A., Shafri, H.Z., 2014. Development of fuzzy rule-based parameters for urban object-oriented classification using very high-resolution imagery. Geocarto Int. 29 (3), 268–292.
Hao, P., Zhan, Y., Wang, L., Niu, Z., Shakir, M., 2015. Feature selection of time series MODIS data for early crop classification using random forest: a case study in Kansas, USA. Remote Sens. (Basel) 7 (5), 5347–5369.
Hay GJ, & Castilla G (2008). Geographic Object-Based Image Analysis (GEOBIA): A new name for a new discipline. In Object-based image analysis: Spatial concepts for knowledge-driven remote sensing applications. Springer Berlin Heidelberg, Berlin, Heidelberg, 75–89.
Haralick, R.M., Shanmugam, K., 1973. Computer classification of reservoir sandstones. IEEE Trans. Geosci. Electron. 11 (4), 171–177.
Immitzer, M., Vuolo, F., Atzberger, C., 2016. First experience with Sentinel-2 data for crop and tree species classifications in central Europe. Remote Sens. (Basel) 8 (3), 166.
Inglada, J., Vincent, A., Arias, M., Marais-Sicre, C., 2016. Improved early crop type identification by joint use of high temporal resolution SAR and optical image time series. Remote Sens. (Basel) 8 (5), 362.
Jaworski, T., Chutkowski, K., 2015. Genesis, morphology, age and distribution of cryogenic mounds on Kaffiøyra and Hermansenøya. Northwest Svalbard. Permafrost and Periglacial Processes 26 (4), 304–320.
Jones, C.G., 2012. Ecosystem engineers and geomorphological signatures in landscapes. Geomorphology 157, 75–87.
Khatami, R., Mountrakis, G., Stehman, S.V., 2016. A meta-analysis of remote sensing research on supervised pixel-based land-cover image classification processes: General guidelines for practitioners and future research. Remote Sens. Environ. 177, 89–100.
Kunz, N.S., Hoffman, M.T., Weber, B., 2012. Effects of heuweltjies and utilization on vegetation patterns in the Succulent Karoo, South Africa. J. Arid Environ. 87, 198–205.
Levick, S.R., Asner, G.P., Kennedy-Bowdoin, T., Knapp, D.E., 2010. The spatial extent of termite influences on herbivore browsing in an african savanna. Biol. Conserv. 143 (11), 2462–2467.
Lim, J.S., Gleason, S., Williams, M., Linares Matás, G.J., Marsden, D., Jones, W., 2021. UAV-Based remote sensing for managing alaskan native heritage landscapes in the Yukon-Kuskokwim delta. Remote Sens. (Basel) 14 (3), 728.
Liu, M.W., Ozdogan, M., Zhu, X., 2013. Crop type classification by simultaneous use of satellite images of different resolutions. IEEE Trans. Geosci. Remote Sens. 52 (6), 3637–3649.
Lovitt, J., Rahman, M.M., McDermid, G.J., 2017. Assessing the value of UAV photogrammetry for characterizing terrain in complex peatlands. Remote Sens. (Basel) 9 (7), 715.
Makinde, E.O., Salami, A.T., Olaleye, J.B., Okewusi, O.C., 2016. Object-based and pixel-based classification using rapideye satellite imager of ETI-OSA, Lagos. Nigeria. Geoinformatics FCE CTU 15 (2), 59–70.

Mali, B., Okello, S., Ocaido, M., Nalule, A.S., 2018. Indigenous knowledge on ecosystem services and management of termites among rural communities in Uganda's rangelands. Livest. Res. Rural. Dev. 30 (2).
Maxwell, A.E., Warner, T.A., Fang, F., 2018. Implementation of machine-learning classification in remote sensing: an applied review. Int. J. Remote Sens. 39 (9), 2784–2817.
McAllister, E., Payo, A., Novellino, A., Dolphin, T., Medina-Lopez, E., 2022. Multispectral satellite imagery and machine learning for the extraction of shoreline indicators. Coast. Eng. 174, 104102.
McAuliffe, J.R., Hoffman, M.T., McFadden, L.D., Bell, W., Jack, S., King, M.P., Nixon, V., 2019. Landscape patterning created by the southern harvester termite, Microhodotermes viator: Spatial dispersion of colonies and alteration of soils. J. Arid Environ. 162, 26–34.
Menze, B.H., Ur, J.A., 2012. Mapping patterns of long-term settlement in Northern Mesopotamia at a large scale. Proc. Natl. Acad. Sci. 109 (14), 778–787.
Mesner, N., Oštir, K., 2014. Investigating the impact of spatial and spectral resolution of satellite images on segmentation quality. J. Appl. Remote Sens. 8 (1), 083696.
Midgley, G., Hoffman, T., 1991. Heuweltjies: nutrient factories. Veld & Flora 77 (3), 72–75.
Myburgh, G., Van Niekerk, A., 2013. Effect of feature dimensionality on object-based land cover classification: a comparison of three classifiers. South African Journal of Geomatics 2 (1), 13–27.
Naylor, L.A., Viles, H.A., Carter, N.E.A., 2002. Biogeomorphology revisited: looking towards the future. Geomorphology 47 (1), 3–14.
Ngcofe, L., Semoli, B., 2022. The status of aerial photogrammetry in South Africa: a transition to digital imagery system. South African Journal of Geomatics 11 (1).
Piazza, G.A., Vibrans, A.C., Liesenberg, V., Refosco, J.C., 2016. Object-oriented and pixel-based classification approaches to classify tropical successional stages using airborne high–spatial resolution images. Giscience & Remote Sensing 53 (2), 206–226.
Picker, M.D., Hoffman, M.T., Leverton, B., 2007. Density of Microhodotermes viator (Hodotermitidae) mounds in southern Africa in relation to rainfall and vegetative productivity gradients. J. Zool. 271 (1), 37–44.
Sales, J.C., Bueno, G.T., Rosolen, V., Ferreira, M.E., Furlan, L.M., 2021. The structure of an earth-mound field of the Brazilian Savanna. Geomorphology 386, 107752.
Sărășan, A., Ardelean, A.C., Bălărie, A., Wehrheim, R., Tabaldiev, K., Akmatov, K., 2020. Mapping burial mounds based on UAV-derived data in the Suusamyr Plateau, Kyrgyzstan. Journal of Archaeological Science 123, 105251.
Shabalala AN &, Ekolu SO (2019). Quality of water recovered by treating acid mine drainage using pervious concrete adsorbent. Water SA 45(4): 638-647.
Singh A, Thakur N, & Sharma A (2016). A review of supervised machine learning algorithms. In 2016, the 3rd International Conference on Computing for Sustainable Global Development (INDIACom), 1310–1315.
Talukdar, S., Singha, P., Mahato, S., Pal, S., Liou, Y.A., Rahman, A., 2020. Land-use land-cover classification by machine learning classifiers for satellite observations—A review. Remote Sens. (Basel) 12 (7), 1135.
Whiteside, T.G., Boggs, G.S., Maier, S.W., 2011. Comparing object-based and pixel-based classifications for mapping savannas. Int. J. Appl. Earth Obs. Geoinf. 13 (6), 884–893.
Yao, Z., Zhao, Y., Wang, H., Li, H., Yuan, X., Ren, T., Yu, L., Liu, Z., Zhang, X., Li, S., 2023. Comparison and Assessment of Data sources with Different Spatial and Temporal Resolution for Efficiency Orchard Mapping: Case Studies in five Grape-growing Regions. Remote Sens. (Basel) 15 (3), 655.
Zheng, B., Myint, S.W., Thenkabail, P.S., Aggarwal, R.M., 2015. A support vector machine to identify irrigated crop types using time-series Landsat NDVI data. Int. J. Appl. Earth Obs. Geoinf. 34, 103–112.